Available online at www.sciencedirect.com
SCIENCE DIRECT®
International Journal of Solids and Structures 43 (2006) 393–412
INTERNATIONAL JOURNAL OF SOLIDS and STRUCTURES
www.elsevier.com/locate/ijsolstr

Vibration and dynamic buckling of shear beam-columns on elastic foundation under moving harmonic loads

Seong-Min Kim [a,1], Yoon-Ho Cho [b,*]

[a] College of Architecture and Civil Engineering, Kyung Hee University, 1 Seocheon-ri, Kiheung-eup, Yongin, Kyunggi 449-701, Republic of Korea
[b] Department of Civil and Environmental Engineering, Chung-Ang University, 221 Huksuk-dong, Dongjak-ku, Seoul 156-756, Republic of Korea

Received 7 September 2004; received in revised form 7 June 2005
Available online 27 July 2005

Abstract

The vibration and buckling of an infinite shear beam-column, which considers the effects of shear and the axial compressive force, resting on an elastic foundation have been investigated when the system is subjected to moving loads of either constant amplitude or harmonic amplitude variation with a constant advance velocity. Damping of a linear hysteretic nature for the foundation was considered. Formulations in the transformed field domains of time and moving space were developed, and the response to moving loads of constant amplitude and the steady-state response to moving harmonic loads were obtained using a Fourier transform. Analyses were performed to examine how the shear deformation of the beam and the axial compression affect the stability and vibration of the system, and to investigate the effects of various parameters, such as the load velocity, load frequency, shear rigidity, and damping, on the deflected shape, maximum displacement, and critical values of the velocity, frequency, and axial compression. Expressions to predict the critical (resonance) velocity, critical frequency, and axial buckling force were proposed.

Keywords: Axial compression; Beam-column; Buckling; Elastic foundation; Frequency; Harmonic load; Moving load; Resonance; Stability; Shear beam; Velocity

* Corresponding author. Tel.: +82 2 820 5336; fax: +82 2 816 0251.
E-mail addresses: seongmin@khu.ac.kr (S.-M. Kim), yhcho@cau.ac.kr (Y.-H. Cho).
[1] Tel.: +82 31 201 3795; fax: +82 31 202 8854.

0020-7683/$ - see front matter © 2005 Elsevier Ltd. All rights reserved.
doi:10.1016/j.ijsolstr.2005.06.025

1. Introduction

To investigate the dynamic response of pavement systems subjected to moving loads, beams and plates on an elastic foundation have widely been employed as the models of the pavement systems (Kim and Roesset, 1998; Liu and Gazis, 1999; Liu et al., 2000; Kim et al., 2002; Kim and McCullough, 2003). When those systems are analyzed with moving loads, the effects of shear and the forces in the plate's in-plane or beam's axial direction are normally ignored. However, asphalt mixtures of the flexible pavement systems are very sensitive to shear and the shear deformations in the thick cement concrete slabs of the rigid pavement systems may not be negligible. Moreover, most rigid pavement systems are subjected to in-plane compressive forces due to environmental loads such as changes in temperature and moisture. If temperature increases, concrete slabs expand and compressive forces are induced because the slabs push each other. Due to these in-plane compressive forces, the concrete pavements sometimes experience buckling, which is also called blowup (Kerr and Dallis, 1985). Blowups are observed both in jointed concrete pavements and continuously reinforced concrete pavements. The in-plane compressive forces are also induced in prestressed concrete pavements (Brunner, 1975; Cable et al., 1986; Powers and Zaniewski, 1987; Okamoto and Tayabji, 1995). Failures of the prestressed concrete pavements caused by high compressive forces sometimes occur. Therefore, the effects of shear and the in-plane compressive forces in the pavement systems need to be investigated when they are subjected to moving loads.

The load amplitude of the moving loads is often assumed to be constant. However, the moving loads created by vehicles in fact have variations in load amplitude with time that result from the pavement surface roughness and the mechanical systems of the vehicles (Nasim et al., 1991; Kim et al., 2002; Kim and McCullough, 2003). In addition, nondestructive testing vehicles such as the rolling dynamic deflectometer apply a steady-state harmonic force while continuously moving (Bay et al., 1995; Kim et al., 1999). The moving loads with such variations in load amplitude need to be considered in addition to the moving loads of constant amplitude. Since the dynamic responses of the pavement systems and their simplified models such as beams and plates on an elastic foundation show similar trends under moving loads (Kim and Roesset, 1997), it is efficient to use beams on an elastic foundation to predict general behaviors of those systems and to investigate the effects of shear and axial compression when they are subjected to moving loads.

The objective of this paper is to discuss the stability and dynamic displacement response of an infinite shear beam on an elastic foundation when the system is subjected to a static axial compressive force and lateral moving loads of either constant amplitude or harmonic amplitude variation. Beams considering the effect of shear and subjected to axial compression and lateral loads are called shear beam-columns. The geometry and material properties were assumed to be linearly elastic. The elastic foundation was considered as either a Winkler-type or a two-parameter foundation and damping of a linear hysteretic or a viscous nature was considered for the foundation. A distributed load with a constant advance velocity was considered instead of a point load because moving loads in practice have normally a finite area over which they are distributed and the point load represents only an extreme case. Formulations in the transformed field domains were developed and the solutions were obtained using a double Fourier transform in time and moving space for moving loads with arbitrary load variation, and a Fourier transform in moving space for the steady-state response to moving harmonic loads and for the response to moving loads of constant amplitude. Analyses were performed to investigate the effects of various parameters, such as the load velocity, load frequency, shear rigidity, and damping, on the displacements and critical values of the velocity, frequency, and axial compressive force, and to examine how the consideration of shear and axial compression affect the displacement response and stability of the system. By conducting a large number of parametric studies, equations to predict the resonance velocity, resonance frequency, and axial buckling force were developed.

2. Formulations

If a shear beam resting on an elastic foundation is subjected to a static axial force and a dynamic vertical load, as shown in Fig. 1, the governing differential equation for the system without damping and ignoring rotary inertia can be written in a Cartesian coordinate system $\{x, y\}$ as

$$m\frac{\partial^2 y(x,t)}{\partial t^2} - S\left[\frac{\partial^2 y(x,t)}{\partial x^2} - \frac{\partial \phi(x,t)}{\partial x}\right] - P\frac{\partial^2 y(x,t)}{\partial x^2} + ky(x,t) = q(x,t), \tag{1}$$

$$EI\frac{\partial^2 \phi(x,t)}{\partial x^2} + S\left[\frac{\partial y(x,t)}{\partial x} - \phi(x,t)\right] = 0, \tag{2}$$

where m is the mass of the beam per unit length, P is the axial force (positive and negative signs represent tension and compression, respectively), k is the stiffness of the foundation per unit length, $q(x,t)$ is the vertical load per unit length, E is Young's modulus of elasticity, I is the second moment of inertia, $y(x,t)$ is the vertical displacement of the beam, $\phi(x,t)$ is the rotation of the beam, and S is the shear rigidity of the beam defined by

$$S = k'AG, \tag{3}$$

where $k'A$ is the effective shear area and G is the shear modulus of the beam.

If the vertical load moves in the positive x direction with a constant advance velocity V, a moving coordinate η can be defined by $x - Vt$. Then, the governing differential equation in a moving Cartesian coordinate system $\{\eta, y\}$ can be expressed as

$$m\left[\frac{\partial^2 y(\eta,t)}{\partial t^2} - 2V\frac{\partial^2 y(\eta,t)}{\partial t\,\partial \eta} + V^2\frac{\partial^2 y(\eta,t)}{\partial \eta^2}\right] - S\left[\frac{\partial^2 y(\eta,t)}{\partial \eta^2} - \frac{\partial \phi(\eta,t)}{\partial \eta}\right] - P\frac{\partial^2 y(\eta,t)}{\partial \eta^2} + ky(\eta,t) = q(\eta,t), \tag{4}$$

$$EI\frac{\partial^2 \phi(\eta,t)}{\partial \eta^2} + S\left[\frac{\partial y(\eta,t)}{\partial \eta} - \phi(\eta,t)\right] = 0. \tag{5}$$

The solutions of Eqs. (4) and (5) can be obtained using the Fourier transform if the beam is assumed to extend to infinity. If ξ and Ω are assumed to be the transformed fields of η (moving space) and t (time), respectively, and if $y(\eta,t)$, $\phi(\eta,t)$, and $q(\eta,t)$ are written in the form of $Y(\xi,\Omega)e^{i\Omega t}e^{i\xi\eta}$, $\Phi(\xi,\Omega)e^{i\Omega t}e^{i\xi\eta}$, and $Q(\xi,\Omega)e^{i\Omega t}e^{i\xi\eta}$, respectively, the transformed displacements $Y(\xi,\Omega)$ and the transformed rotations $\Phi(\xi,\Omega)$ can be obtained by

$$Y(\xi,\Omega) = \frac{Q(\xi,\Omega)}{P\xi^2 + k - m(\Omega - V\xi)^2 + S\xi^2\left(1 - \frac{S}{EI\xi^2+S}\right)}, \tag{6}$$

$$\Phi(\xi,\Omega) = \frac{iS\xi}{EI\xi^2 + S}Y(\xi,\Omega), \tag{7}$$

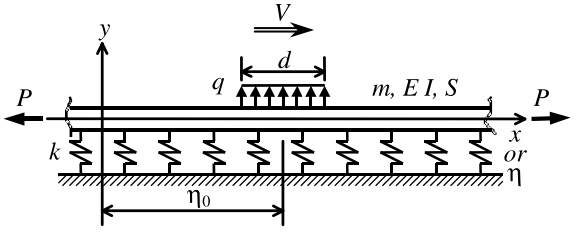

Fig. 1. Shear beam-column on elastic foundation subjected to moving load.

where $\mathrm{i} = \sqrt{-1}$ and the transformed load $Q(\xi, \Omega)$ is obtained using the double Fourier transform

$$Q(\xi, \Omega) = \int_{-\infty}^{\infty} \int_{-\infty}^{\infty} q(\eta, t) \mathrm{e}^{-\mathrm{i}\xi\eta} \mathrm{e}^{-\mathrm{i}\Omega t} \, \mathrm{d}\eta \, \mathrm{d}t. \tag{8}$$

Finally, the dynamic displacement response can be obtained using the double inverse Fourier transform

$$y(\eta, t) = \frac{1}{(2\pi)^2} \int_{-\infty}^{\infty} \int_{-\infty}^{\infty} \frac{Q(\xi, \Omega)}{P\xi^2 + k - m(\Omega - V\xi)^2 + S\xi^2\left(1 - \frac{S}{EI\xi^2 + S}\right)} \mathrm{e}^{\mathrm{i}\xi\eta} \mathrm{e}^{\mathrm{i}\Omega t} \, \mathrm{d}\xi \, \mathrm{d}\Omega. \tag{9}$$

In practice, the above equations are solved using the fast Fourier transform (FFT), which is a discrete transform. In the FFT, if the number of transformed points is sufficiently large, the increment of the field of consideration is small enough, and the total length of the field of consideration, which is determined by multiplying the number of transformed points by the increment of the field, is sufficiently large compared with the response region, then the results should be very close to the analytical solutions with the errors that can be negligible. In addition, to successfully perform the FFT in the time and frequency domains, the system should have some damping. However, this requirement can be dropped when using the exponential window method (Kausel and Roesset, 1992; Kim and Roesset, 1997).

If viscous damping is considered, $c\frac{\partial y(x,t)}{\partial t}$ and $c\left(\frac{\partial y(\eta,t)}{\partial t} - V\frac{\partial y(\eta,t)}{\partial \eta}\right)$ should be added in Eqs. (1) and (4), respectively, where c is the viscous damping constant. In addition, if linear hysteretic damping, which produces an energy loss per cycle that is frequency independent, is considered for the foundation, an expression $2\mathrm{i}Dk$ should be added for the damping term, where D is the damping ratio (Foinquinos and Roesset, 1995). In this case, if the sign of the linear hysteretic damping term is made to be consistent with that of the viscous damping term, the effect of hysteretic damping on the response is similar to that of viscous damping. Then, the transformed displacements in Eq. (6) can be rewritten including damping terms as

$$Y(\xi, \Omega) = \frac{Q(\xi, \Omega)}{P\xi^2 + k(1 + 2\mathrm{i}D) - m(\Omega - V\xi)^2 + S\xi^2\left(1 - \frac{S}{EI\xi^2 + S}\right) + \mathrm{i}c(\Omega - V\xi)}. \tag{10}$$

If a two-parameter foundation (Filonenko-Borodich, 1940; Pasternak, 1954; Kerr, 1964; Vlasov and Leontev, 1966) is considered to include the shear stiffness of the foundation, the term having the axial force P in Eq. (1) can be rewritten as

$$-(P + k_2)\frac{\partial^2 y(x, t)}{\partial x^2}, \tag{11}$$

where k_2 is the second parameter of the two-parameter foundation. As can be seen from Eq. (11), the second parameter of the foundation increases the total axial tensile force (when P is in tension) or reduces the total axial compressive force (when P is in compression). Therefore, the total axial force $(P + k_2)$ should be used if the two-parameter foundation is considered.

If the moving load has a harmonic variation of the amplitude $\mathrm{e}^{\mathrm{i}\overline{\Omega}t}$ and only the steady-state response is of interest, the displacement response in Eq. (9) with considering damping terms can be written as

$$y(\eta, t) = \frac{1}{2\pi} \int_{-\infty}^{\infty} \frac{Q(\xi, \Omega)}{P\xi^2 + k(1 + 2\mathrm{i}D) - m(\overline{\Omega} - V\xi)^2 + S\xi^2\left(1 - \frac{S}{EI\xi^2 + S}\right) + \mathrm{i}c(\overline{\Omega} - V\xi)} \mathrm{e}^{\mathrm{i}\xi\eta} \, \mathrm{d}\xi \tag{12}$$

with

$$Q(\xi, t) = \mathrm{e}^{\mathrm{i}\overline{\Omega}t} \int_{-\infty}^{\infty} q(\eta) \mathrm{e}^{-\mathrm{i}\xi\eta} \, \mathrm{d}\eta, \tag{13}$$

where $\overline{\Omega}$ is the frequency of the moving harmonic load in radians per second. If the response to the force $\sin \overline{\Omega} t$ (the imaginary component of $e^{i\overline{\Omega}t}$ is considered, the imaginary component of Eq. (12) should be used. If a moving load has constant amplitude ($\overline{\Omega} = 0$ in a moving harmonic load), the response can be obtained by inserting 0 into the load frequency $\overline{\Omega}$ in Eqs. (12) and (13). Because η is a point on the moving axis, the above equations represent the response at a moving point with time. The response at a fixed point can simply be determined by the relation $\eta = x - Vt$, where x is the abscissa of the fixed point.

If a moving load has a loaded length d, the load pressure (load per unit length) q, and the variation in load amplitude $qf(t)$, the transformed load Q defined in Eqs. (8) and (13) can be obtained, respectively, by

$$Q(\xi, \Omega) = 2q \frac{\sin \frac{d\xi}{2}}{\xi} e^{-i\xi\eta_0} \int_{-\infty}^{\infty} f(t) e^{-i\Omega t} \, dt, \tag{14}$$

$$Q(\xi, t) = 2q \frac{\sin \frac{d\xi}{2}}{\xi} e^{i\overline{\Omega}t} e^{-i\xi\eta_0}, \tag{15}$$

where η_0 is the coordinate of the center of the load. The transformed load defined in Eq. (14) can be obtained using FFT if the integration that includes the loading function $f(t)$ cannot be solved analytically. If the transient response to the moving harmonic load due to the initial application of the load is also of interest, Eq. (14) should be used instead of Eq. (15) and the harmonic load should be defined from the intended time of application. It is noted that the response including the transient response converges to the steady-state response if there is damping in the system. In this study, when solving Eq. (12) using the FFT, the number of transformed points of 16,384 and the distance increment of 12.7 mm were used.

3. Behavior under a moving load of constant amplitude

The dynamic displacement response and stability under a moving load of constant amplitude (when the load frequency $\overline{\Omega}$ is 0) is investigated first. The material properties and geometry used in this study are listed in Table 1. The values of the parameters not shown in the table, such as load velocity, axial compression, shear rigidity, and damping value, are considered within wide ranges. Damping of a linear hysteretic nature for the foundation is considered in this study.

3.1. Deflected shapes

If a beam is sufficiently long and subjected to a moving load of constant amplitude with a constant advance velocity, the deflected shape under the moving load is the same at any instant along the moving axis. This means that the deflected shape is moving with the load.

The deflected shapes along the moving axis for various values of the shear rigidity are shown in Fig. 2, when a load velocity is 50 m/s, an axial compression is 2 MN, and there is no damping. The 0 distance in

Table 1
Properties of shear beam-column on elastic foundation and moving load

Properties of shear beam-column on elastic foundation	
EI	363.35 kN m^2
m	297.5 kg/m
k	77.17 MPa
Properties of moving load	
Total load	−40 kN
d	0.1524 m
q	−262.5 kN/m

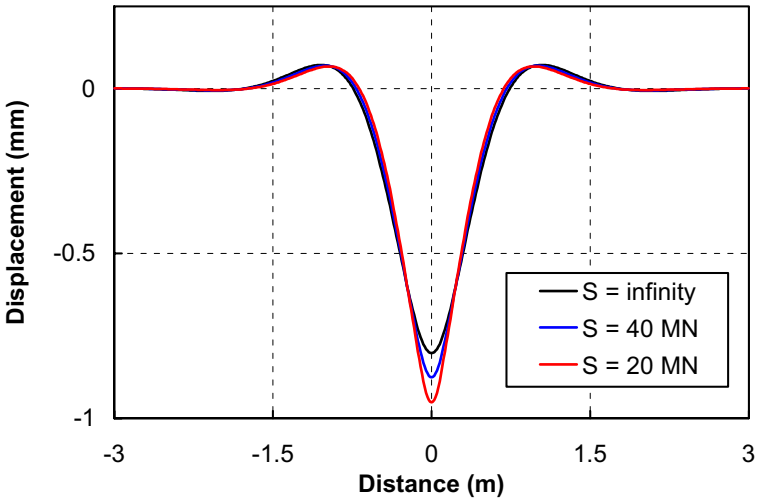

Fig. 2. Deflected shapes when $V = 50$ m/s, $P = -2$ MN, $D = 0$.

the figure represents the location of the center of the load. The deflected shapes are symmetric with respect to the center of the moving load. As the shear rigidity decreases, the maximum deflection becomes larger but the peaks at the front and rear of the moving load are not much affected. It should be noted that the infinite shear rigidity in the figure implies that there is no shear distortion. In this case, the shear beam becomes the Bernoulli–Euler beam. When there is damping in the system, the effect of shear on the deflected shapes is the same as that when there is no damping; however, damping reduces the maximum deflection.

3.2. Critical velocity and buckling force

The effect of the shear rigidity on the relationship between the maximum deflection and the load velocity is shown in Fig. 3. As the load velocity increases, the maximum deflection increases until the velocity becomes close to the critical velocity and then decreases again. The critical velocity decreases as the shear rigidity decreases. For velocities smaller than the critical velocities, the maximum deflection increases as the shear rigidity decreases at a given velocity, which is the case shown in Fig. 2. For velocities larger than the critical velocity of the system that has an infinitely large shear rigidity (in other words, no shear distortion), the maximum deflection at a given velocity decreases with a decrease in the shear rigidity. However, as the velocity increases further, the differences in the maximum deflections become smaller.

The relationships among the critical values of the velocity, shear rigidity, and axial compression are shown in Fig. 4. If two variables are selected from the three variables of velocity, shear rigidity, and axial compression, the critical value of the other variable can be determined by reading the coordinate of the intercept with the critical surface. At a given shear rigidity, as the velocity increases, the critical axial compressive force (buckling force) decreases. At a given velocity, as the shear rigidity decreases, the critical axial compression becomes smaller. At a given axial compression, as the shear rigidity decreases, the critical velocity decreases.

To find the expressions for the critical velocity and the critical axial compressive force, a number of parametric studies were performed considering wide ranges of variables. It was found that the loaded length, within the practical range of the tire print length, did not affect the critical velocity. It was also found that the critical velocity tended to increase very slightly with an increase in the hysteretic damping ratio, but the

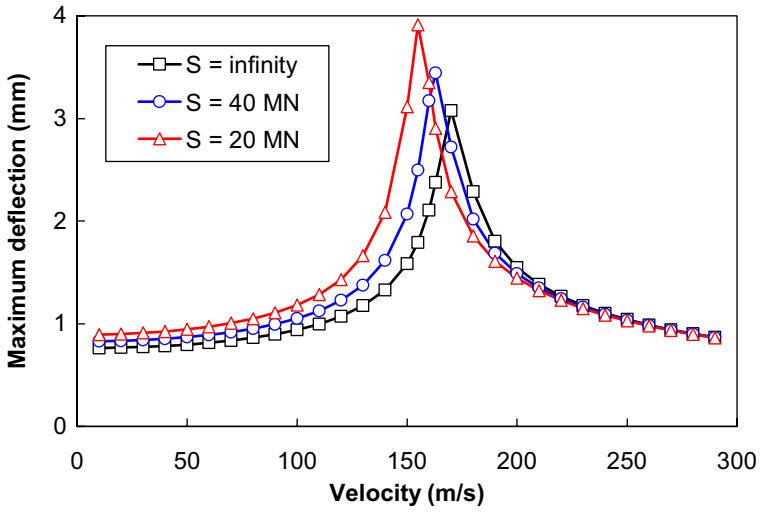

Fig. 3. Relationship between maximum deflection and velocity ($D = 5\%$, $P = -2$ MN).

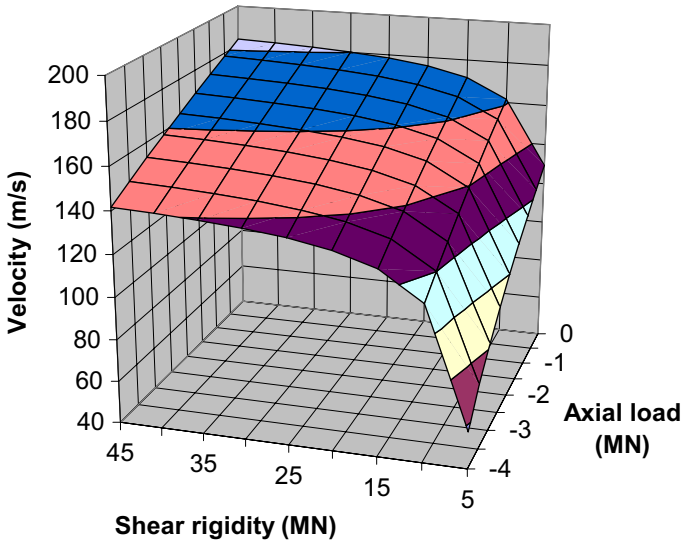

Fig. 4. Relationship among critical values of velocity, axial load, and shear rigidity.

increase was small enough to be negligible within the practical range of the damping ratio for the foundation. Finally, the critical velocity V_{cr0} for a given axial compression and a shear rigidity can be predicted by

$$V_{cr0} = \sqrt{\frac{1}{m}\left(2\sqrt{EIk} + P - \frac{EIk}{S}\right)}. \tag{16}$$

The critical axial compressive force for a given velocity and a shear rigidity can be obtained by solving Eq. (16) for P. Then,

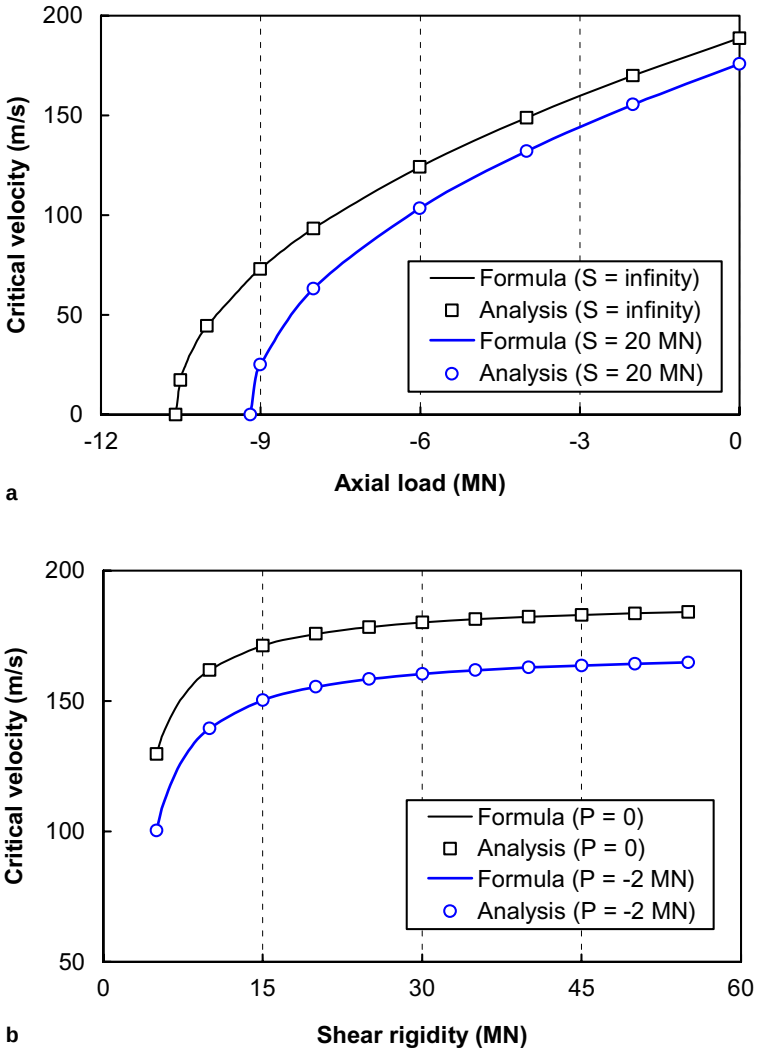

Fig. 5. Comparison of critical velocities from analysis and formula for various values of (a) axial load, and (b) shear rigidity.

$$P_{\mathrm{cr}} = mV^2 - 2\sqrt{EIk} + \frac{EIk}{S}. \tag{17}$$

As can be predicted with Eq. (17), the static buckling force (when $V = 0$) is $-2\sqrt{EIk} + EIk/S$ (the negative sign represents compression). Fig. 5 shows the relationships between the critical velocity and the axial compression, and between the critical velocity and the shear rigidity, obtained from the analysis and predicted by Eq. (16). The results from the analysis and the formula are identical.

4. Behavior under a moving load with harmonic variation

The dynamic displacement response and buckling of a shear beam-column on an elastic foundation is investigated when subjected to a moving load with harmonic amplitude variation. The stability and

vibration of the system for a stationary harmonic load ($V = 0$) are studied first. Then, the displacement amplitude distributions and the maximum displacements under a moving harmonic load are examined for various values of the velocity, load frequency, axial compression, and shear rigidity.

4.1. Vibration and stability under a stationary harmonic load

The relationship between the maximum displacement and the load frequency for a stationary harmonic load ($V = 0$) is shown in Fig. 6. When there is no axial compression, as shown in Fig. 6a, the maximum displacement increases until the load frequency reaches the critical (resonance) frequency and then decreases. The critical frequency is not affected by the shear rigidity. In presence of an axial compressive force, as shown in Fig. 6b, two critical frequencies are observed. The first critical frequency becomes smaller as the

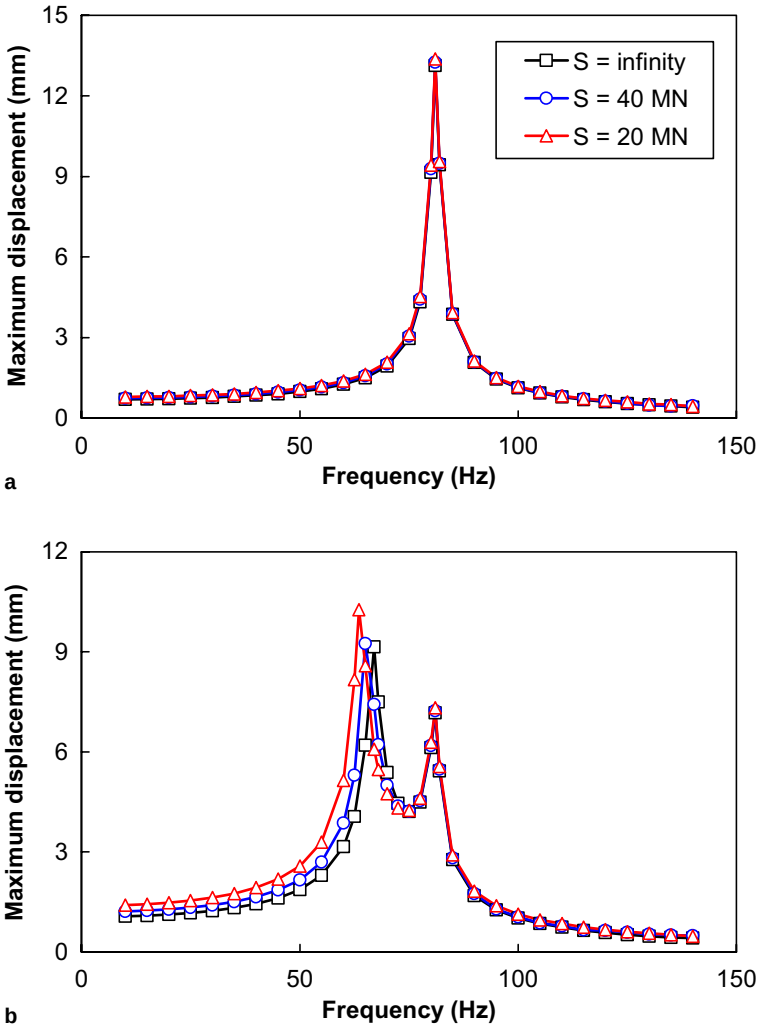

Fig. 6. Relationship between maximum displacement and load frequency for stationary harmonic load: (a) $P = 0$, and (b) $P = -6$ MN ($D = 1\%$).

shear rigidity decreases; however, the second critical frequency is not affected by the shear rigidity and is the same as the critical frequency of the system without axial compression (compare with Fig. 6a). For a given frequency smaller than the first critical frequency, the maximum displacement increases with decreasing the shear rigidity; however, for frequencies larger than the second critical frequency, the maximum displacement does not seem to be affected by the shear rigidity and the effect of shear can be negligible.

The relationships among the critical values of the load frequency, axial compression, and shear rigidity for the stationary harmonic load are shown in Fig. 7. At a given shear rigidity, the critical frequency increases as the axial compression decreases. At a given axial compression (except 0 axial load), the critical

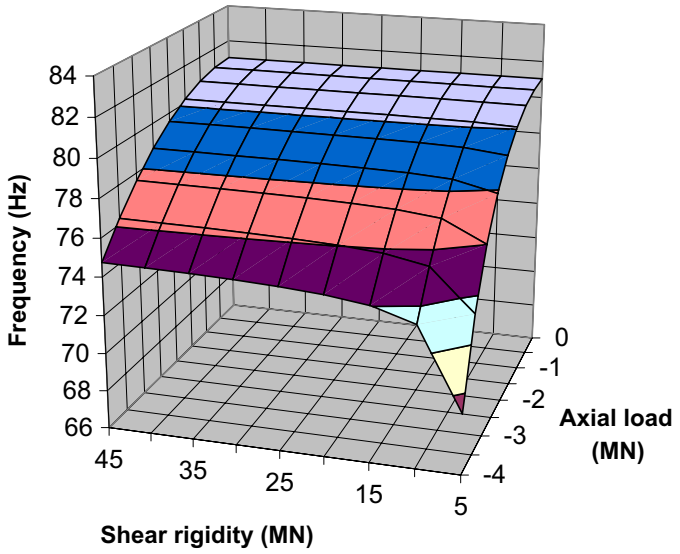

Fig. 7. Relationship among critical values of frequency, axial load, and shear rigidity for stationary harmonic load.

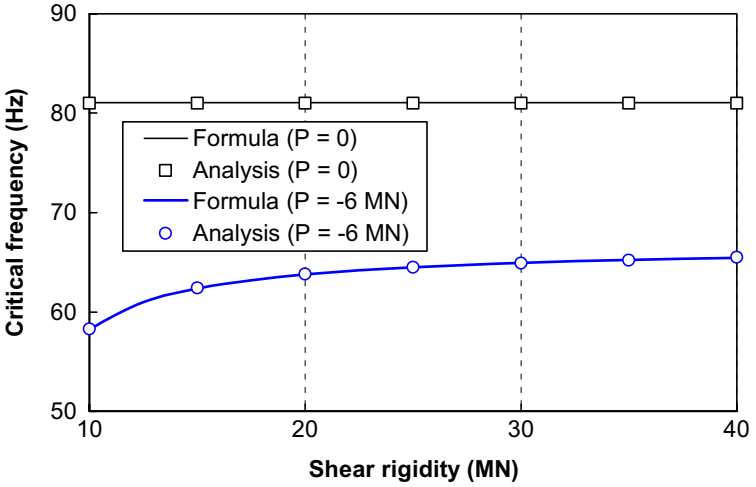

Fig. 8. Comparison of critical frequencies from analysis and formula for stationary harmonic load.

frequency decreases as the shear rigidity decreases. When there is no axial load, the critical frequency is constant regardless of the shear rigidity. At a given frequency, the critical axial compression decreases as the shear rigidity decreases.

From a number of parametric studies, it was found that the critical frequency was affected by many parameters but independent of the loaded length and damping ratio. The first critical frequency in Hz (cps) of the stationary harmonic load, f_{cr0}, can be obtained by

$$f_{cr0} = \frac{1}{2\pi}\sqrt{\frac{k}{m}} \quad (\text{when } P = 0), \tag{18}$$

$$f_{cr0} = \frac{1}{2\pi}\sqrt{\frac{k}{m} - \frac{S(P+2S) - 2S\sqrt{S(P+S)}}{mEI}}. \tag{19}$$

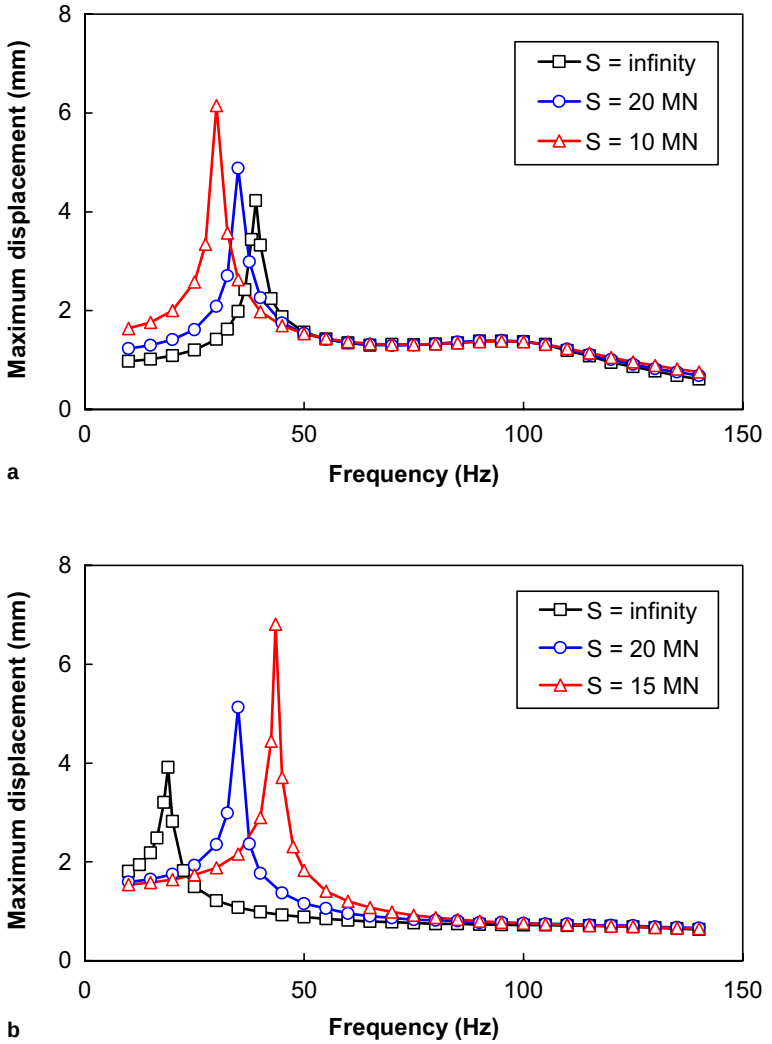

Fig. 9. Relationship between maximum displacement and load frequency ($D = 1\%$, $P = -2$ MN): (a) $V = 100$ m/s, and (b) $V = 200$ m/s.

The second critical frequency is the same as the critical frequency of the system without the axial load and can be determined by Eq. (18). The critical axial compression for a stationary harmonic load can be obtained by rearranging Eq. (19) for P and expressed as

$$P_{\mathrm{cr}} = \frac{EI(k - 4\pi^2 m\bar{f}^2)}{S} - 2\sqrt{EI(k - 4\pi^2 m\bar{f}^2)} \quad \left(\text{when } \bar{f} \leqslant \frac{1}{2\pi}\sqrt{\frac{k}{m}}\right), \tag{20}$$

where $\bar{f}$ is the frequency of the harmonic load in Hz. Fig. 8 shows the relationship between the critical frequency and the shear rigidity for a stationary harmonic load with different axial forces, obtained from the analysis and Eqs. (18) and (19). The results from the analysis and the formulas are identical.

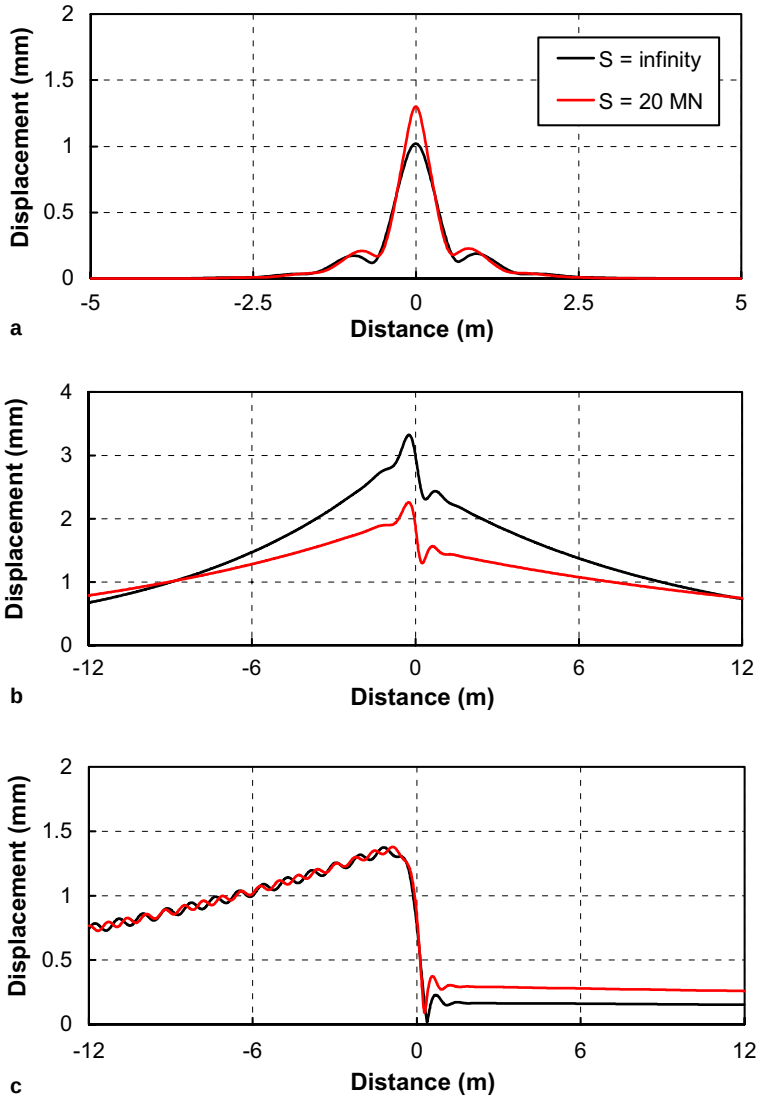

Fig. 10. Displacement distributions for $V = 100$ m/s ($P = -2$ MN, $D = 1$ %): (a) load frequency = 15 Hz, (b) 40 Hz, and (c) 100 Hz.

4.2. Vibration and stability under a moving harmonic load

Fig. 9a shows the relationship between the maximum displacement and the load frequency of the moving harmonic load for a load velocity of 100 m/s that is smaller than the critical velocities of the moving load of constant amplitude (in this case, about 170, 155, and 139 m/s for the systems with the shear rigidities of infinity, 20, and 10 MN, respectively). The critical frequency decreases as the shear rigidity decreases. For frequencies somewhat larger than the critical frequency, the maximum displacement tends to increase again very slightly as the frequency increases, but finally decreases again. As shown in Fig. 9b, for a load velocity of 200 m/s that is larger than the critical velocities of the moving load of constant amplitude,

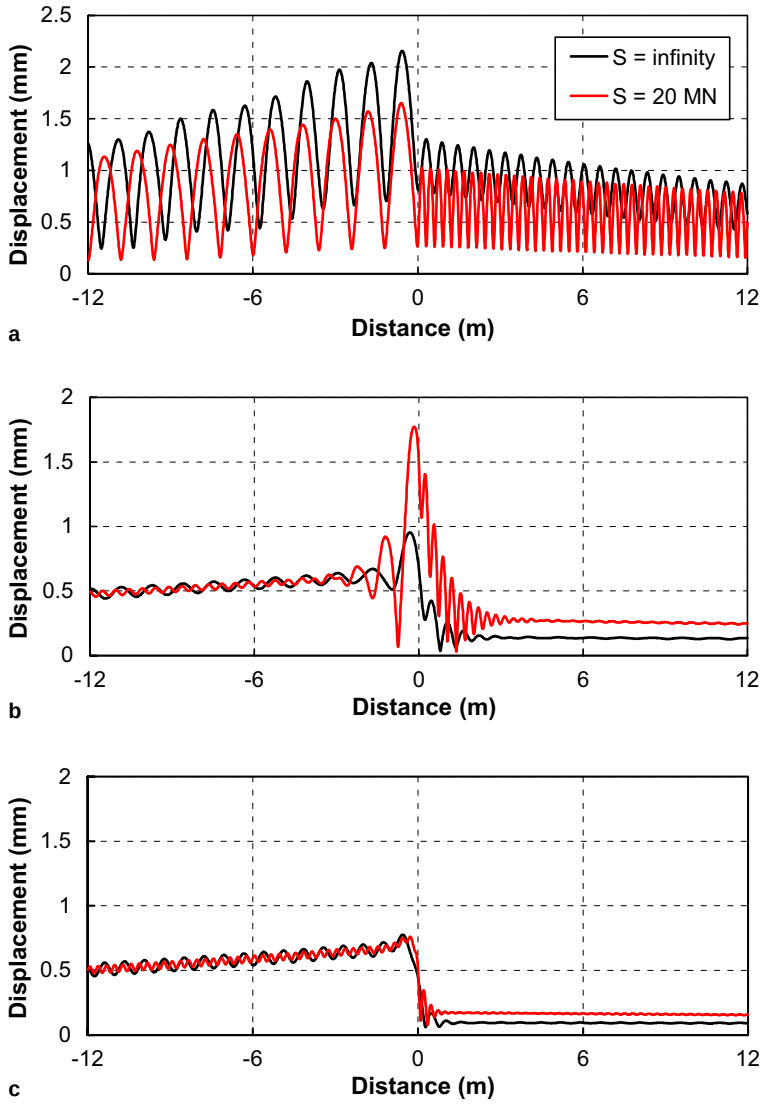

Fig. 11. Displacement distributions for $V = 200$ m/s ($P = -2$ MN, $D = 1\%$): (a) load frequency = 15 Hz, (b) 40 Hz, and (c) 100 Hz.

the critical frequency increases as the shear rigidity decreases. For frequencies larger than the critical frequencies, the differences in the maximum displacements among the systems with different shear rigidities become smaller and can be ignored as the frequency increases.

The displacement amplitude distributions for a moving harmonic load are investigated as shown in Fig. 10 when the load velocity is 100 m/s. Because the response under a moving harmonic load changes with time, the maximum amplitudes of the responses along the moving axis are shown in the figures, and those shapes do not necessarily occur at the same time. As shown in Fig. 10a, when the load frequency is 15 Hz, which is smaller than the critical frequencies (see Fig. 9a), the maximum displacement becomes larger as the shear rigidity decreases. On the other hand, when the load frequency is 40 Hz (Fig. 10b), which is larger than the critical frequencies, the displacement amplitudes decrease with a decrease in the shear rigidity. For a load frequency of 100 Hz (Fig. 10c), the displacement amplitudes in front of the moving load are

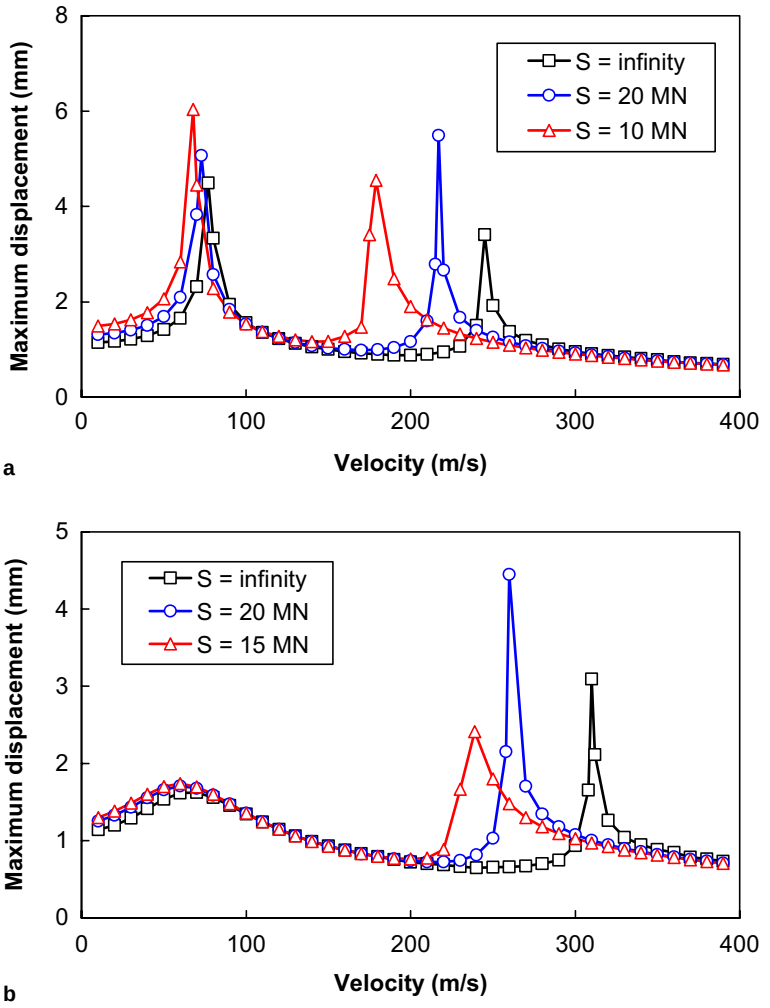

Fig. 12. Relationship between maximum displacement and velocity ($D = 1\%$, $P = -2$ MN): (a) load frequency = 50 Hz, and (b) load frequency = 100 Hz.

significantly smaller than those behind the load. As the shear rigidity decreases, the displacement amplitudes in front of the load increase but those behind the load are not much affected. The maximum displacement does not seem to be affected by the shear rigidity. The distributions of the displacement amplitudes for a load velocity of 200 m/s are shown in Fig. 11. Regardless of the load frequencies, the beam is more stressed behind the moving load. As the shear rigidity decreases, the maximum displacement decreases for a load frequency of 15 Hz (Fig. 11a) but increases for a load frequency of 40 Hz (Fig. 11b), which are the opposite phenomena when the load velocity is 100 m/s. The shapes of the displacement amplitudes for a load frequency of 100 Hz (Fig. 11c) are very similar to those when the load velocity is 100 m/s.

The relationship between the maximum displacement and the load velocity for an axial compression of 2 MN is shown in Fig. 12a when a load frequency is 50 Hz, which is smaller than the first critical frequencies of the stationary harmonic load. There are two critical velocities and both the first and second critical velocities decrease as the shear rigidity decreases. As shown in Fig. 12b, when a load frequency is 100 Hz, which is larger than the second critical frequencies of the stationary harmonic load (in this case, about 81 Hz regardless of the shear rigidity), the peaks corresponding to the second critical velocities are very clearly observed but the peaks corresponding to the first critical velocities are not apparent. The second critical velocity becomes smaller with decreasing the shear rigidity.

The relationship between the critical velocity and the load frequency is shown in Fig. 13. The critical velocity for a load frequency of 0 represents the critical velocity of the moving load of constant amplitude. As the load frequency increases, the first critical velocity decreases until 0 and then increases again for the frequencies larger than the first critical frequency of the stationary harmonic load. However, this re-increase in the first critical velocity after the first critical frequency of the stationary harmonic load tends to disappear for frequencies larger than the second critical frequency of the stationary harmonic load. The second critical velocity increases with an increase in the load frequency. For a given frequency smaller than the first critical frequency of the stationary harmonic load, both the first and second critical velocities decrease as the shear rigidity decreases. For a given frequency larger than the first critical frequency of the stationary harmonic load, the second critical velocity decreases with a decrease in the shear rigidity.

The relationships among the critical values of the frequency, axial compression, and shear rigidity are shown in Fig. 14. When a load velocity is smaller than the critical velocity of the moving load of constant amplitude, as shown in Fig. 14a, at a given shear rigidity, the critical frequency increases as the axial

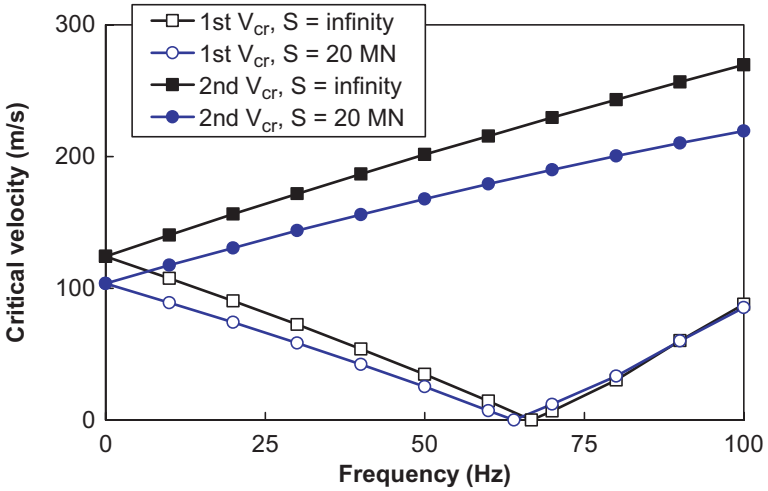

Fig. 13. Relationship between critical velocity and load frequency ($P = -6$ MN).

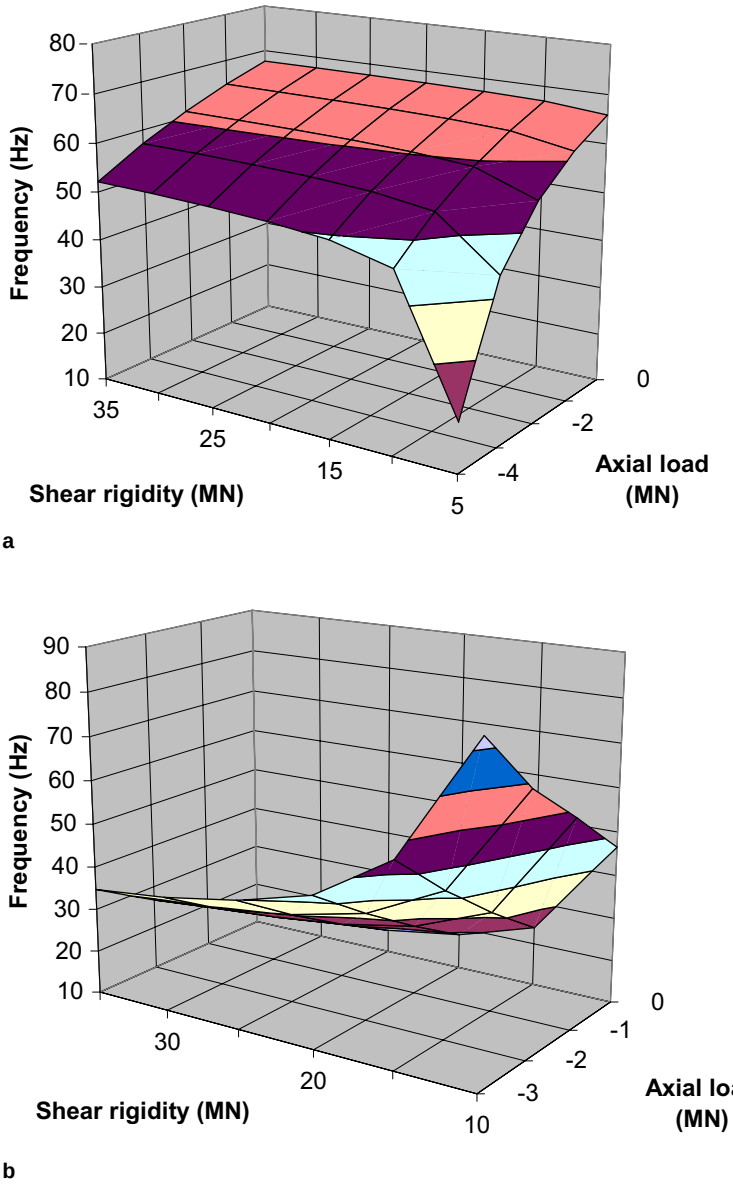

Fig. 14. Relationship among critical values of frequency, axial load, and shear rigidity: (a) $V = 50$ m/s, and (b) $V = 200$ m/s.

compression decreases. At a given axial compression, the critical frequency decreases as the shear rigidity decreases. At a given frequency, the critical axial compressive force decreases as the shear rigidity decreases. When a load velocity is larger than the critical velocity of the moving load of constant amplitude (Fig. 14b), at a given shear rigidity, the critical frequency decreases as the axial compression decreases. At a given axial compression, the critical frequency becomes larger as the shear rigidity decreases. At a given frequency, the critical axial compression decreases with decreasing the shear rigidity, which is the same phenomenon observed with Fig. 14a when the load velocity is smaller than the critical velocity of the moving load of constant amplitude.

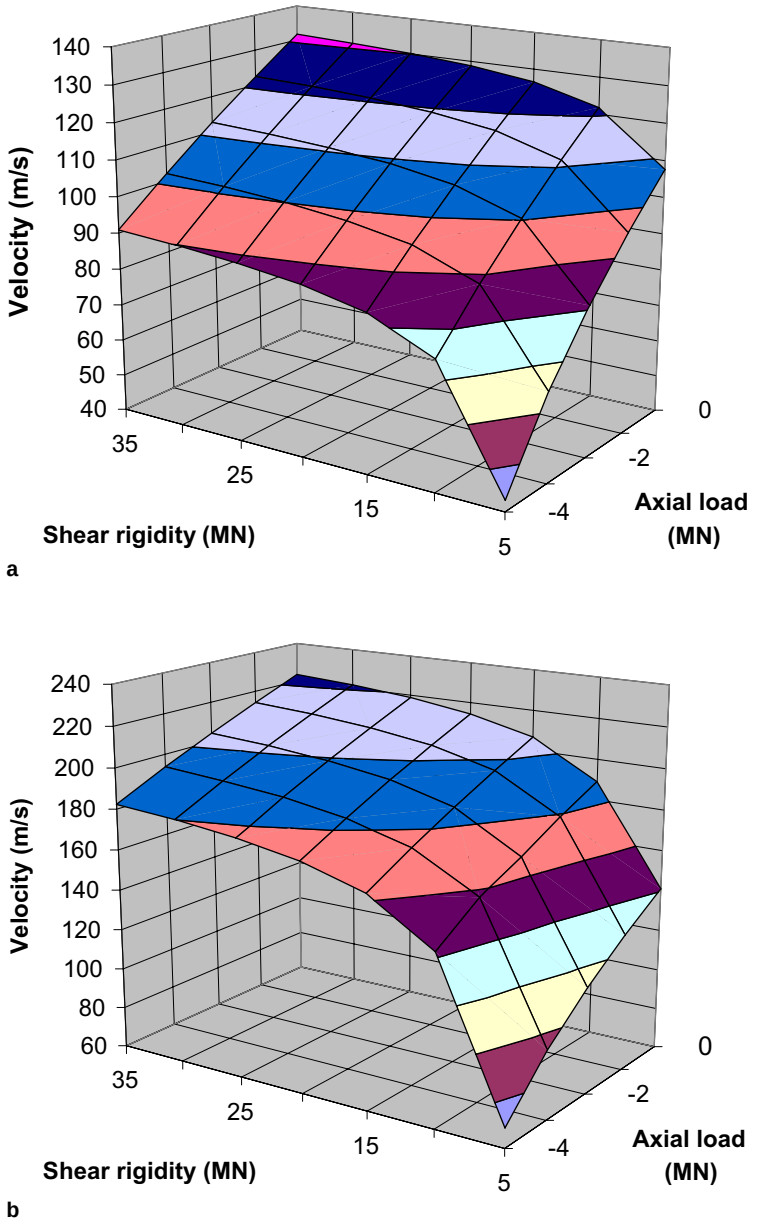

Fig. 15. Relationship among critical values of velocity, axial load, and shear rigidity (load frequency = 30 Hz): (a) first critical velocity, and (b) second critical velocity.

Fig. 15 shows the relationships among the critical values of the velocity, axial compression, and shear rigidity when a load frequency is smaller than the first critical frequency of the stationary harmonic load. For the first critical velocity, as shown in Fig. 15a, at a given shear rigidity, the critical velocity increases as the magnitude of the axial compression decreases. At a given axial compression, the critical velocity decreases with decreasing the shear rigidity. At a given velocity, the critical axial compressive force decreases

as the shear rigidity decreases. For the second critical velocity, as shown in Fig. 15b, the relationships are similar to those for the first critical velocity shown in Fig. 15a. When a load frequency is larger than the first critical frequency of the stationary harmonic load, the first critical velocity tends to disappear as previously mentioned and the relationships among the second critical velocity, axial compression, and shear rigidity are similar to those shown in Fig. 15b.

5. Summary and conclusions

The dynamic displacement response and stability of an infinite shear beam-column resting on an elastic foundation have been investigated when the system is subjected to moving loads of either constant amplitude or harmonic amplitude variation. For the response to moving loads of constant amplitude and for the steady-state response to moving harmonic loads, formulations were developed in the transformed field domains of time and moving space, and solutions were obtained using FFT. Analyses were performed to investigate how the shear rigidity and the axial compression affect the vibration and stability of the system, and to examine the effects of various parameters on the deflected shape, maximum displacement, and critical values of the velocity, frequency, and axial compression. Expressions to predict the critical values of the velocity, frequency, and axial compressive force were proposed. The analysis results point to the following conclusions.

1. When the system is subjected to a moving load of constant amplitude:
   - For velocities smaller than the critical velocity, if the shear effect is considered, the maximum deflection becomes larger as the shear rigidity decreases but the peaks at the front and rear of the load are not much affected.
   - At a given axial compression, the critical velocity decreases as the shear rigidity decreases. At a given shear rigidity, the critical velocity increases with decreasing the axial compression. At a given velocity, the critical axial compression decreases as the shear rigidity decreases.
2. When the system is subjected to a stationary harmonic load:
   - When there is no axial compression, one critical frequency is observed and that is independent of the shear rigidity:
   - In presence of axial compression, two critical frequencies are observed. The first critical frequency is smaller than and the second critical frequency is the same as the critical frequency of the system without considering an axial compression. As the shear rigidity decreases, the first critical frequency decreases but the second critical frequency remains the same regardless of the shear rigidity.
   - At a given shear rigidity, the critical frequency becomes smaller as the axial compressive force increases. In other words, the critical axial compressive force increases as the load frequency decreases. At a given axial compression, the critical frequency decreases with decreasing the shear rigidity. At a given frequency, the critical axial compression becomes smaller as the shear rigidity decreases.
3. When the system is subjected to a moving harmonic load.
   - For velocities smaller than the critical velocity of the moving load of constant amplitude, the critical frequency decreases as the axial compression increases and the shear rigidity decreases. However, for velocities larger than the critical velocity of the moving load of constant amplitude, the critical frequency increases as the axial compression increases and the shear rigidity decreases. Regardless of the velocity, at a given frequency, the critical axial compression decreases as the shear rigidity decreases.

- For frequencies smaller than the first critical frequency of the stationary harmonic load, two critical velocities exist and those critical velocities decrease as the axial compression increases and the shear rigidity decreases. For frequencies larger than the first critical frequency of the stationary harmonic load, the first critical velocity tends to disappear and only the second critical velocity is clearly observed. The second critical velocity also decreases with an increase in the axial compression and a decrease in the shear rigidity.

4. Since the beam on elastic foundation has widely been employed as a simplified model of the pavement systems, the formulations and the analysis results described in this paper can be used to investigate the effects of the shear and the axial compression under the loads imposed by moving vehicles on the behaviors of the pavement systems that are sensitive to the shear deformations, such as asphalt concrete pavements and thick Portland cement concrete pavements, and that are subjected to the axial compression, such as Portland cement concrete pavements and prestressed concrete pavements. In a previous study (Kim and Roesset, 1997), the relationships among the responses of the Euler beam on elastic foundation, the Kirchhoff plate on elastic foundation, and the layered pavement systems subjected to moving loads were identified, and the equations to find the beam width and the vertical stiffness of the foundation were developed when using the Euler beam on elastic foundation to predict the responses of more rigorous models of the pavement systems. The methodology used in that study can also be employed for the shear beam-columns on elastic foundation to predict effects of the shear and the axial force in the pavement systems. An alternative would be to find the percent difference in the responses between the Euler beam and the shear beam-column on elastic foundation and simply to apply the percent difference when considering the pavement response. Further studies, however, need to be conducted in this area.
5. As examined in this paper, neglecting the effects of the shear and the axial compression when the pavement systems are analyzed may provide significant errors in predicting their behaviors. The current AASHTO 2002 design guide for pavement systems does not include the shear and the axial force effects when predicting the behaviors, such as displacements, stresses and cracks, of the pavement systems. Since the performance prediction models of the pavement systems in the design guide are directly affected by the behaviors of the pavement systems, the inclusion of those effects can improve the performance prediction of the pavement systems.

References

Bay, J.A., Stokoe II, K.H., Jackson, J.D., 1995. Development and preliminary investigation of a rolling dynamic deflectometer. Transportation Research Record 1473, 43–54.

Brunner, R.J., 1975. Prestressed pavement demonstration project. Transportation Research Record 535, 62–72.

Cable, N.D., McCullough, B.F., Burns, N.H., 1986. New concepts in prestressed concrete pavement. Transportation Research Record 1099, 1–12.

Filonenko-Borodich, M.M., 1940. Some approximate theories of the elastic foundation (in Russian). Uchenyie Zapiski Moskovskogo Gosudarstuennogo Universiteta Mechanika 46, 3–18.

Foinquinos, R., Roesset, J.M., 1995. Dynamic Nondestructive Testing of Pavements. Geotechnical Engineering Report GR95-4, Geotechnical Engineering Center, The University of Texas at Austin.

Kausel, E., Roesset, J.M., 1992. Frequency domain analysis of undamped systems. ASCE Journal of Engineering Mechanics 118 (4), 721–732.

Kerr, A.D., 1964. Elastic and viscoelastic foundation models. Journal of Applied Mechanics 31 (3), 491–498.

Kerr, A.D., Dallis, W.A., 1985. Blowup of concrete pavements. ASCE Journal of Transportation Engineering 111 (1), 33–53.

Kim, S.-M., McCullough, B.F., 2003. Dynamic response of plate on viscous Winkler foundation to moving loads of varying amplitude. Engineering Structures 25 (9), 1179–1188.

Kim, S.-M., Roesset, J.M., 1997. Dynamic Response of Pavement Systems to Moving Loads. Geotechnical Engineering Report GR97-4, Geotechnical Engineering Center, The University of Texas at Austin.

Kim, S.-M., Roesset, J.M., 1998. Moving loads on a plate on elastic foundation. ASCE Journal of Engineering Mechanics 124 (9), 1010–1016.

Kim, S.-M., Roesset, J.M., Stokoe II, K.H., 1999. Numerical simulation of rolling dynamic deflectometer tests. ASCE Journal of Transportation Engineering 125 (2), 85–92.

Kim, S.-M., Won, M.C., McCullough, B.F., 2002. Dynamic stress response of concrete pavements to moving tandem-axle loads. Transportation Research Record—Journal of the Transportation Research Board 1809, 32–41.

Liu, C., Gazis, D., 1999. Surface roughness effect on dynamic response of pavements. ASCE Journal of Transportation Engineering 125 (4), 332–337.

Liu, C., McCullough, B.F., Oey, H.S., 2000. Response of rigid pavements due to vehicle-road interaction. ASCE Journal of Transportation Engineering 126 (3), 237–242.

Nasim, M.A., Karamihas, S.M., Gillespie, T.D., Hansen, W., Cebon, D., 1991. Behavior of a rigid pavement under moving dynamic loads. Transportation Research Record 1307, 129–135.

Okamoto, P.A., Tayabji, S.D., 1995. Instrumentation and evaluation of prestressed pavement section in Pennsylvania. Transportation Research Record 1505, 103–111.

Pasternak, P.L., 1954. On a new method of analysis of an elastic foundation by means of two foundation constants (in Russian). Gosudarstvennoe Izdatelstvo Literaturi po Stroitelstvu i Arkhitekture, Moscow.

Powers, R.L., Zaniewski, J.P., 1987. Nine-year performance evaluation of Arizona's prestressed concrete pavement. Transportation Research Record 1136, 1–11.

Vlasov, V.Z., Leontev, U.N., 1966. Beams, plates and shells on elastic foundations (translated from Russian). Israel Program for Scientific Translation, Jerusalem, Israel.